

Effect of heat treatment on microstructures and mechanical properties of a bulk nanostructured Al-Zn-Mg-Cu alloy

Han-bin Chen^{1,2)} and Bin Yang¹⁾

1) State Key Laboratory for Advanced Metals and Materials, University of Science and Technology Beijing, Beijing 100083, China

2) No.59 Institute of China Ordnance Industry, Chongqing 400039, China

(Received 2009-01-04)

Abstract: A bulk nanostructured Al-10.0Zn-2.8Mg-1.8Cu alloy was synthesized by cryomilling first and then by spark plasma sintering (SPS), and the effect of heat treatment on the microstructures and mechanical properties of this alloy were studied. Most MgZn₂ particles with a coarse size lie on the grain boundaries of the SPS-processed sample. After solid solution and artificial aging, fine spherical-like MgZn₂ particles precipitate uniformly in the grain interiors. No obvious grain growth is found after the heat treatment. A nanoindentation study indicates that no clear change is found in the Yong's modulus of the nanostructured alloy after the heat treatment. However, the hardness of the nanostructured alloy increases by about 33% after the heat treatment, which is attributed to the effect of precipitation-hardening.

Key words: bulk nanostructured materials; Al-Zn-Mg-Cu alloy; nanoindentation; microstructure; mechanical properties; precipitation-hardening

[This work was financially supported by the National High-Tech Research and Development Program of China (No.2002AA302502).]

1. Introduction

Grain refinement and precipitation-hardening are two key approaches to improve the mechanical properties of some coarse alloys. According to the well-know Hall-Petch equation, there is an increase in strength with a decrease in grain size. The precipitation-hardening in nanostructured alloys is a new field worthy of attentions. Recently, some studies on precipitation-hardening in ultrafine-grained materials have been performed on Al alloys using severe plastic deformation (SPD) combined with heat treatment [1-3]. The effect of second-phase particles on the mechanical properties of the alloys is similar to that in the coarse-grained counterparts. However, there has been little systemic work on the influence of second-phase particles on the mechanical properties of nanostructured alloys, and the underlying mechanism associated with the effect of second-phase particles in the nanostructured matrix is not understood.

The nanoindentation technique has been widely

used in investigating the mechanical properties of various micromaterials at small scales since last decades [4-5]. Due to the small deforming volume, this technique is used particularly to investigate the hardness, Yong's modulus and the deformation mechanisms of nanostructured or ultrafine-grained metals and alloys [6-8]. The purpose of this paper was to investigate the effect of second-phase particles on the microstructures and mechanical properties of bulk nanostructured Al alloys by nanoindentation and transmission electron microscopy (TEM) techniques.

2. Experimental

As-atomized Al-Zn-Mg-Cu (10.0 Zn, 2.8 Mg, 1.8 Cu, balance Al, wt%) alloy powders with particle sizes of less than 40 μm were the predecessor. The nanocrystalline Al-Zn-Mg-Cu alloy powders were fabricated by mechanical milling in a liquid nitrogen medium, namely cryomilling. The details of this processing method can be found in Ref. [9]. The mill-

ing was performed in an attritor with a ball (6.34 mm in diameter, GCr15 bearing steel)-to-powder ratio of 30:1 for 10 h at a rotation speed of 200 rpm. The resultant nanocrystalline powders were consolidated by spark plasma sintering (SPS) using a SPS-3.20-MK-V SPS apparatus under a vacuum of 10 Pa. The sintering was assisted with a uniaxial pressure of 50 MPa and a heating rate of 100°C/min. The samples were kept at the maximal temperature of 450°C for 120 s. The density of the SPS-processed sample was 2.86 g·cm⁻³, which was about 96% of the counterpart prepared by spray forming. For eliminating the coarse precipitations, some samples were solution treated at 445°C/30 min+470°C/30 min then quenched into ambient water. Subsequently, these samples were immediately aged at 120°C for 12 h.

The quasi-static nanoindentation experiments using one loading-unloading cycle were performed at room temperature using a Nanoindenter II equipped with a Berkovich diamond indenter. The Berkovich diamond indenter was pressed into the surface of specimens up to 500 nm at the strain rate of 0.01 s⁻¹. A displacement control mode was used to obtain the load-displacement (*P-h*) curves. The thermal drift of the nanoindentation equipment was less than 0.2 nm/s. 5 indentation tests at one indentation condition were performed to give the statistic data of the experiment. The microstructure analysis of samples was carried out with a PHILIPS APD-10 X-ray diffractometer equipped with a graphite monochromator using Cu K_α radiation. TEM was performed with a JEM-2010 microscope operating at 160 kV. The TEM thin-foil specimens were prepared by the conventional twin-jet electropolishing technique using a 30vol% nitric acid plus a 70vol% methanol solution at -20°C and 20 V.

3. Results and discussion

3.1. Evolution of second phases

Second phases play an important role in the microstructures and mechanical properties of multiphase alloys. Thereby, the evolution of second phases should be studied during synthesizing and heat treatment of the alloys. Fig. 1 shows the XRD patterns of the samples in different states. It can be seen that the cryomilled alloy powder is characterized by the face-centered cubic supersaturated solid solution, as shown in Fig. 1(a). XRD analysis [10] shows that the extremely small nanocrystalline microstructure with a grain size of about 23 nm forms in the Al alloy powder after cryomilling for 10 h. During the process of consolidating by SPS, the precipitation of the second-phase particles from the supersaturated solid so-

lution and the grain growth occur, as shown in Fig. 1(b). One can see that MgZn₂ peaks are present in the XRD pattern of the alloy. These MgZn₂ particles are coarse and heterogeneous due to the high temperature of SPS, which will be shown later. To enhance the effect of the precipitation-hardening, proper solution treatment and artificial aging should be performed to eliminate these coarse MgZn₂ particles. Fig. 1(c) shows the XRD pattern of the sample after solution treatment at the scheme of 445°C/30 min+470°C/30 min. It can be seen that the diffraction peaks of MgZn₂ phase disappear, indicating that MgZn₂ phase is dissolved into the Al matrix. After artificial aging at 120°C for 12 h, MgZn₂ phase precipitates again, as shown in Fig. 1(d).

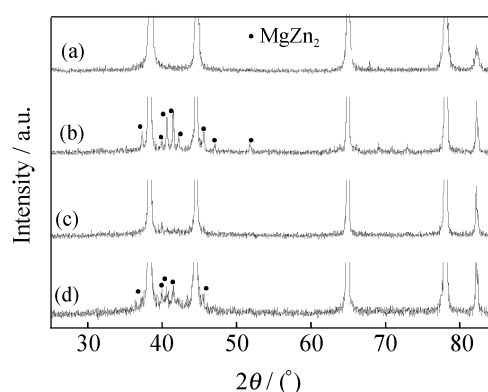


Fig. 1. XRD patterns of samples: (a) as-cryomilled; (b) as-SPS-processed; (c) as-solution-treated; (d) as-aged.

3.2. Microstructures of the nanostructured Al-Zn-Mg-Cu alloy

Fig. 2(a) reveals the typical microstructure of the SPS-processed Al alloy sample, showing that the fine grains with the average grain size of about 200 nm are homogeneously distributed in the matrix. In addition, there are only a few of second-phase particles can be identified in the grain boundaries of the image with a low magnification. Fig. 2(b) shows a magnified microstructure of the SPS-processed sample. There are a larger number of coarse MgZn₂ particles with the size of 50 nm in the grain boundaries, and a few of spherical-like MgZn₂ particles in the grain interiors. Lots of coarse MgZn₂ particles lie on the grain boundaries of the bigger grains. In addition, the distribution of the precipitations in the grain interiors is heterogeneous.

Fig. 3(a) presents the primary microstructure of the heat-treated sample. One can see that the grain size keeps about 200 nm after the heat treatment, showing that the nanostructured Al-Zn-Mg-Cu alloy has a higher thermal stability. The high thermal stability of the nanostructured alloy is related to the pinning effect of second-phase particles on grain boundaries. The visible change is that a lot of MgZn₂ particles precipi-

tate dominantly in the grain interiors rather than on the grain boundaries. This phenomenon can be found obviously in the image with a higher magnification, as shown in Fig. 3(b), in which a lot of fine spherical-like $MgZn_2$ particles are present in the grain interiors. In

addition, some spherical area of moiré fringes with size of about 20 nm can be seen in the same grain interiors, as shown by white arrows, which indicates that some precipitations overlap together.

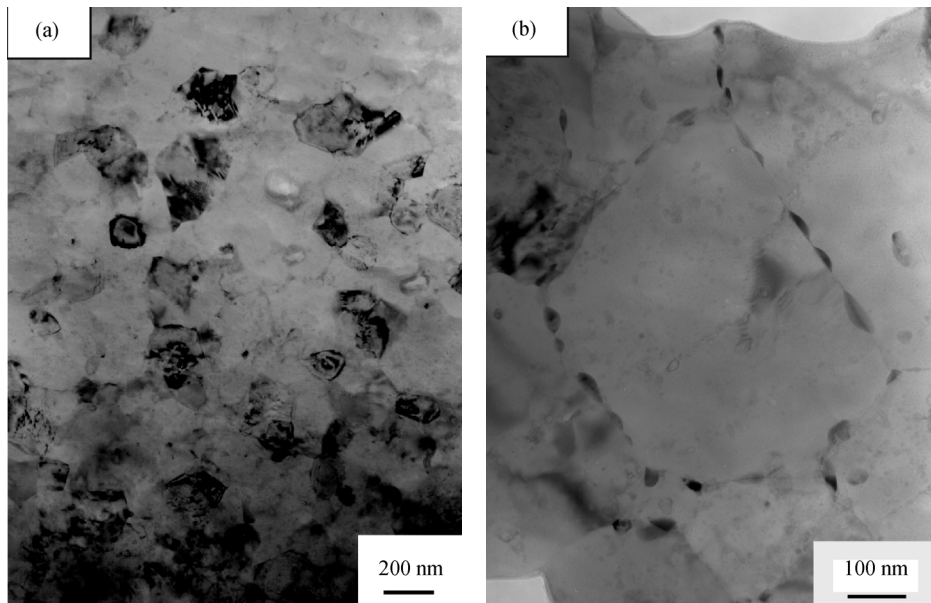


Fig. 2. Microstructures of the SPS-processed nanostructured Al-Zn-Mg-Cu alloy: (a) bright-field image; (b) high magnification image showing distribution of precipitations.

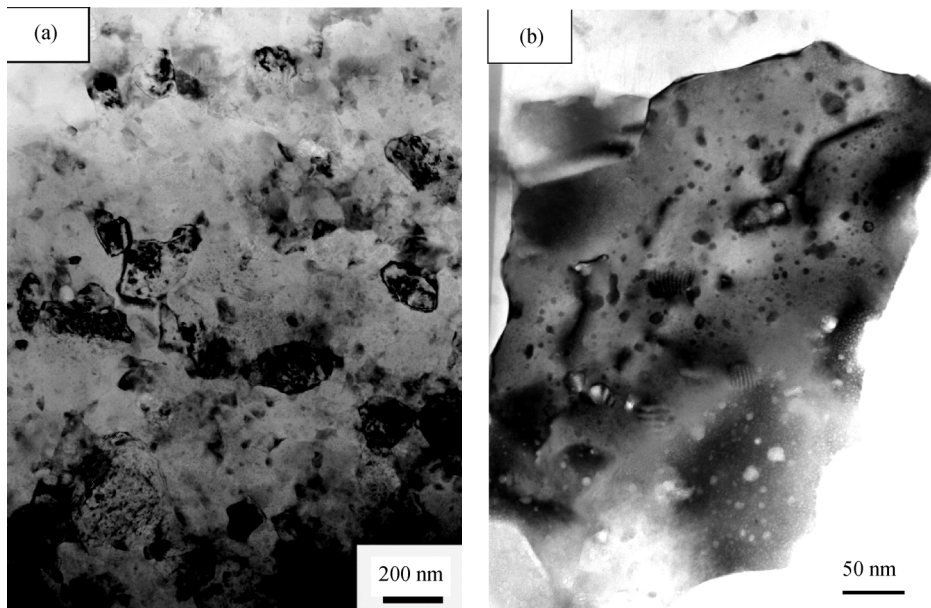


Fig. 3. Microstructures of the aged nanostructured Al-Zn-Mg-Cu alloy: (a) bright-field image; (b) high magnification image showing distribution of precipitations.

The cryomilled powders are in the state of nanocrystal and supersaturated solid solution. Grain growth and precipitation will occur during the following hot consolidation. Joule heat conducted by plasma [11-13] and high density current [14] during the SPS are responsible for the high rate of grain growth and preferable precipitation of coarse $MgZn_2$ particles in the grain boundaries. The grain size is about 200 nm, and lots of coarse $MgZn_2$ particles lie on the grain

boundaries in the SPS-processed samples, as shown in Fig. 2. After solution treatment and aging, the average grain size of the alloy sample prepared by SPS does not change obviously (Fig. 3). Moreover, one can see that a lot of fine spherical-like $MgZn_2$ particles homogeneously precipitate in the grain interiors. Consequently, the remarkable effect of heat treatment on the microstructures of the nanostructured Al-Zn-Mg-Cu alloys is the variation of the distribution and mor-

phology of MgZn_2 particles.

This high thermal stability would be related to the synthetic process and the pinning effect of second phases on the grain boundaries. Experiments show that the formation of oxide and nitride during cryo-milling are responsible for the high thermal stability of nanostructured metals and alloys [15-17] by Zener pinning. However, the pinning effect of the oxide and nitride is limited due to small quantity. Fortunately, the quantity of MgZn_2 particles in the grain boundaries is very large, and the pinning effect of these MgZn_2 particles is very effective [18]. The solute drag at the grain boundaries can also enhance the thermal stability of the alloy, though the pinning effect decreases due to the dissolution of these MgZn_2 particles during the solution treatment.

3.3. Nanoindentation testing

Representative nanoindentation load-displacement curves of the bulk nanostructured Al-Zn-Mg-Cu alloy are shown in Fig. 4. Obviously, the load required to reach the same indentation depth in the heat-treated sample increases gradually. Figs. 5 and 6 show typical curves of Young's modulus and hardness of the bulk nanostructured samples before and after the heat treatment, respectively. No clear change is found in the Young's modulus (E) of the nanostructured alloy after the heat treatment. However, the hardness (H) of the alloy increases obviously after the heat treatment. By averaging measurement data obtained from the indentation depths ranging from 150 to 450 nm, the Young's modulus of the as-SPS-processed sample is found to be 82.7 ± 1.99 GPa, and 81.9 ± 2.93 GPa for the as-aged sample. The propensity of the two values is equivalent with increasing indentation depth. The corresponding values of hardness are 2.17 GPa, and 2.89 GPa, respectively. After the heat treatment, the hardness of the alloy increases by about 33%. The significantly increase in hardness of the alloy should be attributed to the effect of precipitation-hardening, which will be discussed later.

The hardness of the coarse-grained counterpart prepared by spray forming is about 1.7 GPa. According to the Hall-Petch relationship ($H = H_0 + k_H d^{-1/2}$, where H is the hardness, H_0 the inherent hardness, k_H the constant and d the grain size), the hardness of an alloy can be significantly improved when the grain size reaches nanoscale. Falling short of our expectations, the SPS-processed sample does not reveal a high value of hardness, which is only 2.17 GPa. This phenomenon may be explained by the fact that a large number of coarse MgZn_2 particles precipitate on the grain boundaries during the SPS. As a result, most

elements for forming MgZn_2 particles are depleted from the Al grain interiors. The smaller the grain size is, the more the coarse MgZn_2 particles on the grain boundaries are. Consequently, the hardness of the alloy is not as high as supposed.

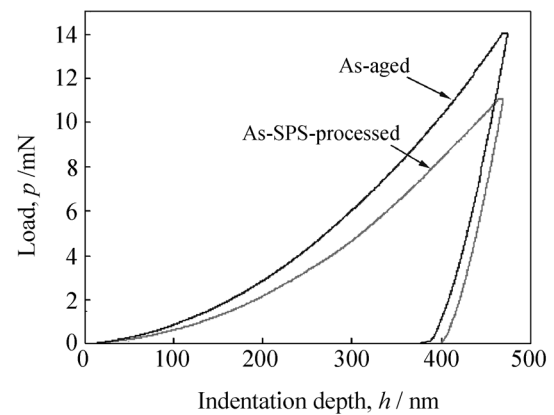


Fig. 4. P - h curves of the SPS-processed and aged nanostructured Al-Zn-Mg-Cu alloys.

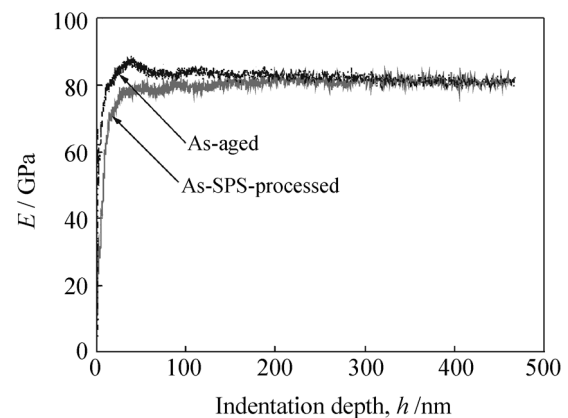


Fig. 5. Young's modulus of the SPS-processed and aged nanostructured Al-Zn-Mg-Cu alloys.

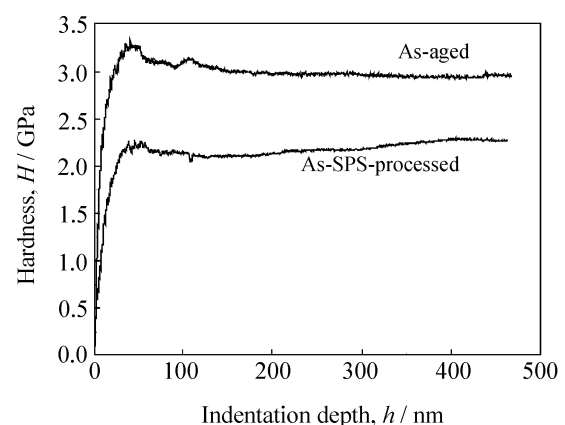


Fig. 6. Hardness of the SPS-processed and aged nanostructured Al-Zn-Mg-Cu alloy.

For obtaining precipitation-hardening effect in nanostructured Al-Zn-Mg-Cu alloys fabricated by SPS, those coarse MgZn_2 particles on the grain boundaries should be dissolved into the nanostructured matrix and redistributed in the grain interiors by an artificial ag-

ing. Fig. 1(c) displays that a supersaturated solid solution is formed after the solution treatment, indicating that the $MgZn_2$ phase is almost dissolved into the Al matrix. $MgZn_2$ particles can be precipitated again during artificial aging. Compared Fig. 2(b) with Fig. 3(b), it can be seen that the location and micrograph of $MgZn_2$ particles in the heat treated sample are obviously different from that in the SPS-processed sample. In the heat treated sample, spherical $MgZn_2$ particles are fine and precipitate homogeneously in the grain interiors rather than on the grain boundaries. Consequently, there are apparent increments of the hardness and the load required to reach the same indentation depth in the heat treated sample. The hardness of the alloy after the heat treatment reaches 2.89 GPa, which is about 33% larger than that (2.17 GPa) of the alloy before the heat treatment. The experimental results show that the effect of precipitation-hardening in the nanostructured Al-10.0Zn-2.8Mg-1.8Cu alloys is significant.

4. Conclusions

(1) The typical microstructure of the SPS-processed nanostructured Al alloy is composed of equiaxed grains with an average grain size of 200 nm. No obvious grain growth is found after the solution treatment and aging. The high grain size stability can be related to the solute drag and the pinning effect of $MgZn_2$ in the grain boundaries.

(2) Most $MgZn_2$ particles with a coarse size lie on the grain boundaries for the SPS-processed nanostructured Al-10.0Zn-2.8Mg-1.8Cu alloy. After solid solution and artificial aging, fine spherical-like $MgZn_2$ particles precipitate uniformly in the grain interiors.

(3) Heat treatment can remarkably enhance the hardness of the bulk nanostructured aluminum alloys. The values of the heat treated and the SPS-processed samples are 2.89 GPa and 2.17 GPa, respectively, which can be attributed to precipitation-hardening in the nanostructured Al-10.0Zn-2.8Mg-1.8Cu alloys.

References

- [1] Y.H. Zhao, X.Z. Liao, Z. Jin, R.Z. Valiev, and Y.T. Zhu, Microstructures and mechanical properties of ultrafine grained 7075 Al alloy processed by ECAP and their evolutions during annealing, *Acta Mater.*, 52(2004), p.4589.
- [2] L.J. Zheng, C.Q. Chen, T.T. Zhou, P.Y. Liu, and M.G. Zeng, Structure and properties of ultrafine-grained Al-Zn-Mg-Cu and Al-Cu-Mg-Mn alloys fabricated by ECA pressing combined with thermal treatment, *Mater. Charact.*, 49(2002), p.455.
- [3] Y.H. Zhao, X.Z. Liao, S. Cheng, E. Ma, and Y.T. Zhu, Simultaneously increasing the ductility and strength of nanostructured alloys, *Adv. Mater.*, 18(2006), p.2280.
- [4] W.C. Oliver and G.M. Pharr, Measurement of hardness and elastic modulus by instrumented indentation: advance in understanding and refinements to methodology, *J. Mater. Res.*, 19(2004), p.13.
- [5] C.A. Schuh, Nanoindentation studies of materials, *Mater. Today*, 9(2006), p.32.
- [6] A. Concustell, J. Sort, S. Surinach, A. Gebert, J. Eckert, A.P. Zhilyaev, and M.D. Baro, Severe plastic deformation of a Ti-based nanocomposite alloy studied by nanoindentation, *Intermetallics*, 15(2007), p.1038.
- [7] Y. Choi, W.Y. Choo, and D. Kwon, Analysis of mechanical property distribution in multiphase ultra-fine-grained steels by nanoindentation, *Scripta Mater.*, 45(2001), p.1401.
- [8] J. Gubicza, G. Dirras, P. Szommer, and B. Bacroix, Microstructure and yield strength of ultrafine grained aluminum processed by hot isostatic pressing, *Mater. Sci. Eng. A*, 458(2007), p.385.
- [9] B.Q. Han, D. Matejczyk, F. Zhou, Z. Zhang, C. Bampton, E.J. Lavernia, and F.A. Mohamed, Mechanical behavior of a cryomilled nanostructured Al-7.5 pct Mg alloy, *Metall. Mater. Trans. A*, 35(2004), p.947.
- [10] F. Zhou, X.Z. Liao, Y.T. Zhu, S. Dallek, and E.J. Lavernia, Microstructural evolution during recovery and recrystallization of a nanocrystalline Al-Mg alloy prepared by cryogenic ball milling, *Acta Mater.*, 51(2003), p.2777.
- [11] W. Li and L. Gao, Rapid sintering of nanocrystalline $ZrO_2(3Y)$ by spark plasma sintering, *J. Eur. Ceram. Soc.*, 20(2000), p.2441.
- [12] W. Chen, U. Anselmi-Tamburini, J.E. Garay, J.R. Groza, and Z.A. Munir, Fundamental investigations on the spark plasma sintering/synthesis process: I. Effect of dc pulsing on reactivity, *Mater. Sci. Eng. A*, 394(2005), p.132.
- [13] S. Paris, E. Gaffet, F. Bernard, and Z.A. Munir, Spark plasma synthesis from mechanically activated powders: A versatile route for producing dense nanostructured iron aluminides, *Scripta Mater.*, 50(2004), p.691.
- [14] J. Ye, L. Ajdelsztjn, and J.M. Schoenung, Bulk nanocrystalline aluminum 5083 alloy fabricated by a novel technique: cryomilling and spark plasma sintering, *Metall. Mater. Trans. A*, 37(2006), p.2569.
- [15] R.J. Perez, B. Huang, and E.J. Lavernia, Thermal stability of nanocrystalline Fe-10wt% Al produced by cryogenic mechanical alloying, *Nanostruct. Mater.*, 7(1996), p.565.
- [16] B. Huang, R.J. Perez, and E.J. Lavernia, Grain growth of nanocrystalline Fe-Al alloys produced by cryomilling in liquid argon and nitrogen, *Mater. Sci. Eng. A*, 255(1998), p.124.
- [17] V.L. Tellkamp, S. Dallek, D. Cheng, and E.J. Lavernia, Grain growth behavior of a nanostructured 5083Al-Mg alloy, *J. Mater. Res.*, 16(2001), p.938.
- [18] V.Y. Novikov, Grain growth controlled by mobile particles on grain boundaries, *Scripta Mater.*, 55(2006), p.243.